Relevant long-range interaction of the entanglement Hamiltonian emerges from a short-range gapped system

Chuhao Li,[1,2] Rui-Zhen Huang,[3] Yi-Ming Ding,[4,5,6] Zi Yang Meng,[7] Yan-Cheng Wang,[8,9,*] and Zheng Yan[5,6,†]

[1]*Beijing National Laboratory for Condensed Matter Physics and Institute of Physics, Chinese Academy of Sciences, Beijing 100190, China*
[2]*School of Physical Sciences, University of Chinese Academy of Sciences, Beijing 100190, China*
[3]*Department of Physics and Astronomy, Ghent University, Krijgslaan 281, S9, B-9000 Ghent, Belgium*
[4]*State Key Laboratory of Surface Physics and Department of Physics, Fudan University, Shanghai 200438, China*
[5]*Department of Physics, School of Science and Research Center for Industries of the Future, Westlake University, Hangzhou 310030, China*
[6]*Institute of Natural Sciences, Westlake Institute for Advanced Study, Hangzhou 310024, China*
[7]*Department of Physics and HKU-UCAS Joint Institute of Theoretical and Computational Physics, The University of Hong Kong, Pokfulam Road, Hong Kong SAR, China*
[8]*Hangzhou International Innovation Institute, Beihang University, Hangzhou 311115, China*
[9]*Tianmushan Laboratory, Hangzhou 311115, China*

(Received 5 October 2023; revised 9 May 2024; accepted 9 May 2024; published 31 May 2024)

Beyond the Li-Haldane-Poilblanc conjecture, we find the entanglement Hamiltonian (EH) is actually not closely similar to the original Hamiltonian on the virtual edge. Unexpectedly, the EH has some relevant long-range interacting terms which hugely affect the physics. Without loss of generality, we study a spin-$1/2$ Heisenberg bilayer to obtain the entanglement information between the two layers through our newly developed quantum Monte Carlo scheme, which can simulate large-scale EH. Although the entanglement spectrum carrying the Goldstone mode seems like a Heisenberg model on a single layer, which is consistent with Li-Haldane-Poilblanc conjecture, we demonstrate that there actually exists a finite-temperature phase transition of the EH. The results violate the Mermin-Wagner theorem, which means there should be relevant long-range terms in the EH. It reveals that the Li-Haldane-Poilblanc conjecture ignores necessary corrections for the EH which may lead totally different physics.

DOI: 10.1103/PhysRevB.109.195169

I. INTRODUCTION

Quantum entanglement is a powerful tool to extract and characterize the informational, field-theoretical, and topological properties of quantum many-body systems [1–4], which combines the conformal field theory (CFT) and the categorical description of the problem [5–17]. Low-lying entanglement spectrum (ES) has been widely employed as a fingerprint of CFT and topology in the investigation in highly entangled quantum matter [18–36].

Besides the famous gapped phase in the spin-integer antiferromagnetic Heisenberg chain as Haldane's conjecture [37,38], there is another well-noted Haldane's conjecture about the relationship between the entanglement spectrum and edge energy spectrum. More than one decade ago, Li and Haldane creatively pointed out the ES may be a more precise physical quantity rather than entanglement entropy (EE) [39]. Furthermore, they demonstrated that the general $\nu = 5/2$ topological states have the same low-lying ES to identify the topology and CFT structure. In addition, they predicted that the ES of the topological state would be very similar to the energy spectrum of the edge state, that is, the Li-Haldane conjecture (Haldane's conjecture for ES). The ES is defined as the energy spectrum of the corresponding entanglement Hamiltonian (EH). If a total system is separated into subsystem A and environment $\bar{A}$, then the EH of A, i.e., H_A, can be written as $H_A = -\ln \rho_A$, where the $\rho_A = \mathrm{Tr}_{\bar{A}}(\rho)$ is the reduced density matrix (RDM) of the subsystem A.

The conjecture seems not only limited to the topological states. Two years later, Poilblanc pointed out, via numerical results, that the relation between the low-lying ES and edge energy spectrum exists generally in quantum spin systems beyond topological states [40]. Thereafter, the conjecture has also been called as Li-Haldane-Poilblanc conjecture and extended into general cases beyond topological systems. Then, Qi, Katsura, and Ludwig theoretically proved the general relationship between ES of $(2+1)d$ gapped topological states and the spectrum on their $(1+1)d$ edges exactly when the edge is a CFT [21].

Recent studies have explored the EH in greater depth, using a combination of field theory, numerical simulations, and experimental data [41–56]. The correspondence between edge and entanglement spectra has been successfully applied to many quantum states of matter with topological properties [28,57–59]. Previous studies on a one-dimensional (1D) system implies the EH might not strictly be a short-range one, but instead involves long-range interactions characterized by exponential decay. Remarkably, these long-range interactions appear to have little impact on the short-range entanglement dynamics. The low-lying ES in these systems shows

*ycwangphys@buaa.edu.cn
†zhengyan@westlake.edu.cn

similarities with both the EH and the edge energy spectrum, leading us to consider that the long-range terms of the entanglement Hamiltonian might be insignificant and can potentially be ignored for an approximate analysis [44,60].

Given that the EH and the edge Hamiltonian have been considered comparable in many contexts, it is reasonable to expect that they share fundamental physical properties. At a minimum, their basic features should exhibit similarities. However, whether the seemingly useless long-range terms are indeed irrelevant is still ignored under the conventional wisdom.

Meanwhile, the influence of long-range interactions has been widely studied in past decades [61–68]. It is well known that the long-range interactions $\sim\frac{1}{r^\alpha}$ are irrelevant when the decaying power is large. Otherwise, the long-range terms indeed change the intrinsic physics, e.g., violating the Mermin-Wagner theorem [69,70] even then destroying the Goldstone mode in continuous symmetry breaking systems [71–75]. Thus the Mermin-Wagner theorem is a good standard to check whether the long-range interaction is relevant. The difficulty lies in how to extract the information of the EH in a $(2+1)d$ entangled system. It was extremely challenging for previous numerical methods, such as exact diagonalization (ED) and density matrix renormalization group (DMRG) algorithms due to the limited system sizes. We note the authors of Ref. [76] pointed out the existing thermal phase transition for EH to question the universality of the ES. However, the discussion in the reference is still located in the region of Mermin-Wagner theorem and defaults to the EH are short ranged.

Recently, two of the authors proposed a numerical scheme by designing an nth Rényi RDM $\rho_A^n = e^{-n\mathcal{H}_A}$ within the path-integral frame to capture the information of the entanglement spectrum $\mathcal{H}_A$ by treating the large n as an effective imaginary time length β_A (reciprocal of temperature). A replica partition function of nth Rényi RDM $\mathcal{Z}_A^{(n)} = \mathrm{Tr}[\rho_A^n] = \mathrm{Tr}[e^{-n\mathcal{H}_A}]$ was constructed and can be simulated via quantum Monte Carlo (QMC) [32–34,77]. More details to calculate the ES from the QMC can be found in Ref. [77]. In that method, the n is fixed in a large value to simulate the imaginary time evolution of the EH. Inspired by it, we find the finite-temperature information of EH can be obtained by the QMC if we set the n as a variable. Thus the problem proposed above can now be studied.

II. MODEL

To demonstrate the relevant difference between the edge Hamiltonian and the EH, we take a $S = 1/2$ antiferromagnetic Heisenberg model on a bilayer square lattice as an example. The Hamiltonian can be written as

$$H = J_{\mathrm{in}} \sum_{\langle ij\rangle} (\boldsymbol{S}_{i,1}\boldsymbol{S}_{j,1} + \boldsymbol{S}_{i,2}\boldsymbol{S}_{j,2}) + J_\perp \sum_i \boldsymbol{S}_{i,1}\boldsymbol{S}_{i,2}, \quad (1)$$

where J_{in} denotes the intralayer interaction constant and $J_\perp$ denotes the interlayer interaction constant. Here the $\boldsymbol{S}_{i,l}$ is the spin-1/2 operator at site i and layer l ($l = 1, 2$). Each layer is a periodic boundary condition (PBC) square lattice with sites of $N = L \times L$, and $\langle ij\rangle$ represents the intralayer pair of nearest-neighbor sites. We next define $J = J_\perp/J_{\mathrm{in}}$ to reflect the relative strength of the interaction.

TABLE I. The critical Js under different β_A. The high-precision result of critical J under $\beta_A = 1$ comes directly from Ref. [78], as a reference.

β_A	1	2	3	4	5
J	2.5220(1)	8.5(5)	10.0(5)	11.5(5)	13.0(5)

The ground-state phase diagram of such a bilayer model has been well studied in previous works: the $(2+1)d$ $O(3)$ quantum critical point (QCP), separating the Néel phase and interlayer dimerized phase, is found to be located at $J = 2.5220(1)$ from high-precision QMC simulations [15,17,78,79], as shown in the lower part of Fig. 1(a). We choose one layer to be the subsystem A and the other one to be the environment $\bar{A}$. Previous studies hinted that the entanglement Hamiltonian $\mathcal{H}_A$ would resemble a Heisenberg model on the square lattice following the Li-Haldane-Poilblanc conjecture [39,40].

Unexpectedly, we find that there exists a continuous phase transition in the EH at the finite effective temperature T_A. The system undergoes a spontaneous symmetry breaking from high to low temperature. The phase diagram is shown in Fig. 1(c). Our finding suggests that the EH cannot simply be understood as a single-layer Heisenberg model, in which the Mermin-Wagner theorem forbids the spontaneous breaking of continuous symmetries at a finite temperature in a short-range interacting model. However, such a continuous phase transition can happen when the interactions become long range [62,80,81]. Therefore, our results strongly indicate that some important corrections between the EH and the edge Hamiltonian are needed necessarily.

III. METHOD

The central problem is how to simulate the nth Rényi RDM $\mathrm{Tr}[e^{-n\mathcal{H}_A}]$ by QMC. As previous research [77] suggests, $\mathcal{Z}_A^{(n)}$ is a partition function in a replicated manifold, where the time boundaries of region A of the n replicas are connected along imaginary time and the time boundaries of the region $\bar{A}$ of every replica are independent to each other (for sites in $\bar{A}$ for each replica, the usual periodic boundary condition of β is maintained).

We then provide a brief overview of how we applied the simulation method proposed in Ref. [77] to our study. We start by writing the state of the system as $|\alpha_A^i, \alpha_{\bar{A}}^j\rangle$, in which we are using the superscripts $i, j = 0, 1, \ldots, n$ ($n = \beta_A$) to denote the index of the replica and subscripts A and $\bar{A}$ to denote the region. With the trace relationship mentioned above and swapping the order of trace, we now have $Z_A^{(n)} = \mathrm{Tr}[\rho_A^n] = \mathrm{Tr}[(\mathrm{Tr}_{\bar{A}}\rho)^n] = \mathrm{Tr}_{\bar{A}}[(\mathrm{Tr}\rho)^n]$. After expanding the inner trace, we could get

$$\begin{aligned}(\mathrm{Tr}\rho)^n = &\langle\alpha_A^0, \alpha_{\bar{A}}^0|e^{-\beta H}|\alpha_A^1, \alpha_{\bar{A}}^0\rangle\langle\alpha_A^1, \alpha_{\bar{A}}^1|e^{-\beta H}|\alpha_A^2, \alpha_{\bar{A}}^1\rangle\\ &\times \langle\alpha_A^2, \alpha_{\bar{A}}^2|e^{-\beta H}|\alpha_A^3, \alpha_{\bar{A}}^2\rangle\\ &\cdots\langle\alpha_A^i, \alpha_{\bar{A}}^i|e^{-\beta H}|\alpha_A^i, \alpha_{\bar{A}}^{(i-1)}\rangle\\ &\cdots\langle\alpha_A^n, \alpha_{\bar{A}}^n|e^{-\beta H}|\alpha_A^0, \alpha_{\bar{A}}^n\rangle. \end{aligned} \quad (2)$$

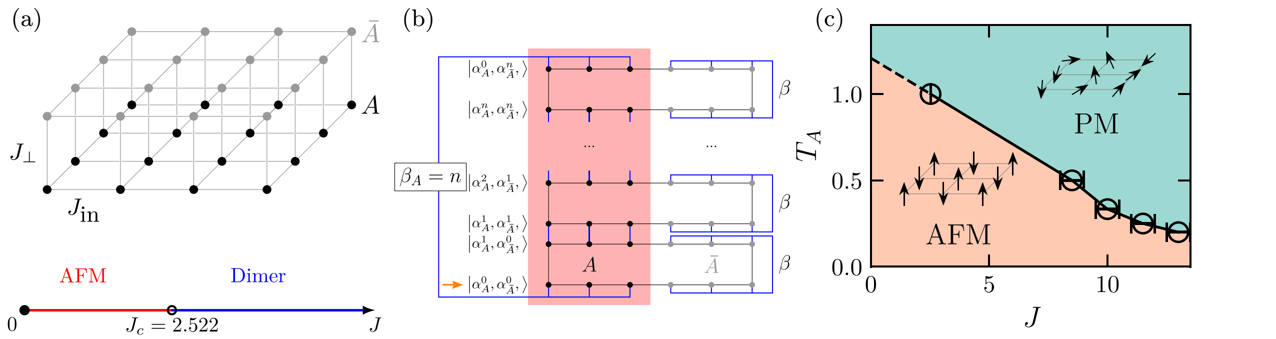

FIG. 1. (a) The lattice of the bilayer Heisenberg model. Darker dots denote sites in the region A we are concerned with. Lighter dots denote sites in the environment $\bar{A}$. The lower part shows the quantum phase diagram of the vanilla bilayer Heisenberg model, which has a quantum phase transition from the AFM phase to tge dimer phase, and its critical point is located at $J_c = 2.522$; the result comes from Refs. [78,79]. (b) An illustration of the replica manifold structure in the imaginary time of the QMC simulation. The blue line indicates the connected spin states which are identical on the edge of the replicas. The spin states in regions A and $\bar{A}$ are connected differently in their own region, and follow a different PBC. The orange arrow indicates the imaginary time to perform the MC measurement. (c) The phase diagram of the entanglement Hamiltonian H_A. The $J = J_\perp/J_{\rm in}$ is the coupling ratio of the original Hamiltonian of the bilayer Heisenberg model. The $T_{\rm A}$ is the effective temperature of the entanglement Hamiltonian H_A, that is, the partition function of the entanglement Hamiltonian is $Z = e^{-H_A/T_{\rm A}}$. The data of the points in the plot are listed in Table I. The point of $T_A = 1$ corresponds to the J_c in the lower parts of (a). The dashed line in (c) is directly extended to $J = 0$ from the segment established by the points of $T_A = 1$ and $T_A = 0.5$.

Noticing that we already utilized the relationship that, at the edge of two adjacent $e^{-\beta H}$ in the imaginary time of region A, $|\alpha_A^i\rangle = |\alpha_A^{(i-1)}\rangle$, and the PBC of region A is maintained as well. The whole process is also depicted as Fig. 1(b).

Therefore, the finite-temperature properties of the EH can be extracted numerically. Here n performs the role of an effective inverse temperature β_A for the EH. In this way, we can readily make use of such an effective imaginary time $\beta_A = n$ at those $n = 1, 2, 3, \ldots,$ integer points to extract the thermal properties of the EH.

It is important to highlight that the term "temperature" can refer to two distinct concepts in this context. The first is the actual temperature T, related to the original Hamiltonian H, with $T = 1/\beta$, and the other one is the effective temperature T_A associated with the EH $\mathcal{H}_A$, where $T_A = 1/\beta_A$. It can be seen that the effective inverse temperature $\beta_A = n$ for the EH $\mathcal{H}_A$ of the subsystem A is in the unit of 1 whereas the $\beta = 1/T$ of the total system is in the inverse unit of the physical energy scale of the original system J of the Heisenberg model, for instance. Here we set the β to be large and allow it to increase proportionally with the system size L to make the system approach its ground state. When discussing the finite-temperature phase transition of the EH $\mathcal{H}_A$, the "temperature" here refers to the T_A $(1/\beta_A)$. In the replica manifold we simulate, the β_A can be tuned by changing the number of replicas n.

As mentioned above, with the expansion form of partition function $\mathcal{Z}_A^{(n)}$, we could then construct a special geometry structure in the stochastic series expansion (SSE) QMC [82–88] to measure those order parameters. All the measurements here are defined in the scope of EH. As an example, for a physical observable O defined on EH and its corresponding partition function $Z_A^{(n)}$, the expectation value $\langle O\rangle_{H_A}$ is given by

$$\langle O\rangle_{H_A} = \mathrm{Tr}\big[\rho_A^n O\big]. \tag{3}$$

Applying the relationship

$$e^{-H_A} = \rho_A = \mathrm{Tr}_{\bar{A}}\rho = \mathrm{Tr}_{\bar{A}}[e^{-\beta H}], \tag{4}$$

one can write it as

$$\langle O\rangle_{H_A} = \mathrm{Tr}[(\mathrm{Tr}_{\bar{A}}[e^{-\beta H}])^n O]. \tag{5}$$

Note that, according to the property of trace calculation, all the measurements about the EH should be done in the connection of the two neighboring replicas [77,89–91]. For simplicity, the physical observables in this work are taken on the $|\alpha_A^0\rangle$ as the arrow points out in Fig. 1(b).

IV. RESULTS

Since we established the basic method, we then perform the simulation with 12 independent processes. Each process executes 5000 MC steps of warming up and the measurement value is averaged over 20 bins, with 10 000 MC steps in each. The result is then averaged by those 12 results.

A. Finite-temperature phase transition of the EH

First, we measure the order parameter $\langle m^2\rangle = \langle(\frac{1}{N}\sum_{i=1}^N \phi_i S_{i,1}^z)^2\rangle$, where $\phi_i = (-1)^{x_i+y_i}$. Then from the magnetization operator, we can also calculate the corresponding second Binder ratio R_2 for the order parameter of the EH, which is defined as $R_2 = \langle m^4\rangle/\langle m^2\rangle^2$.

Considering our method is limited to the discrete β_A, we next fix the β_A and scan the continuous J to obtain better precision results. Therefore, the finite-temperature phase transition points at fixed β_A can be calculated much more accurately. The results of the Binder ratio R_2 under $\beta_A = 3$ are shown in Fig. 2(a) as an example, within the length of system size $L = 8, 16, 24, 32$. From Fig. 2(a), we can locate the critical point at $J = 10.0(5)$ under $\beta_A = 3$. Then a calculation sweeping integer β_A (n) is then carried with same system

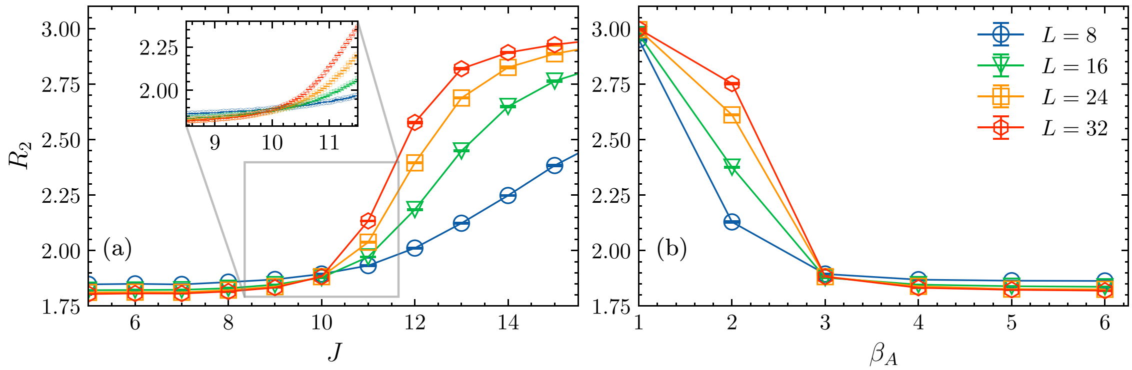

FIG. 2. The Binder ratio R_2 results of different L (a) under $\beta_A = 3$ sweeping J and (b) under $J = 10.0$ sweeping β_A. The crossing point in (a) indicates a phase transition nearing $J = 10.0$. The inset in (a) shows more detailed data around the crossing point, ranging from $J = 8.5$ to $J = 11.5$ and spacing with 0.05. While using $J = 10.0$ in (b), the crossing point locates at $\beta_A = 3$ approximately, which also proves the existence of the phase transition. All calculations are under low real temperature $\beta = 2 \times L$.

size's configurations, to show that those curves indeed cross at $\beta_A = 3$, as an additional proof. The results are plotted in Fig. 2(b).

The finite-temperature phase transition point of the EH at $\beta_A = 1$ is the same as the QCP of the original Hamiltonian at zero temperature. They share the same $J_c \sim 2.52$. From the quantum phase transition view, this criticality is a $(2+1)d$ $O(3)$ class. It implies that the corresponding two-dimensional (2D) thermal dynamical phase transition of the EH should involve others (relevant long-range terms) to make it seem like a $(2+1)d$ criticality.

We also expand the calculation of the Binder ratio R_2 to other β_As; those results at $\beta_A = 2, 3, 4, 5$ are shown as Fig. 3. Then we could locate those β_A's corresponding critical Js and arrange them as the table in Table I. These data points form the phase diagram of the EH shown in Fig. 1(c).

B. Stable order of the EH at low temperature

Due to the limit of the integer β_A, the finite-temperature phase transition may not be solid enough via the above evidence in the readers' opinions. Hereby, through fixing the $\beta_A = 3$, we carefully calculate the order parameter under different coupling ratio J and system sizes L, as shown in Fig. 4(a) with double logarithmic axes. Here we also set the original reciprocal-temperature β scales with system size L where $\beta = 2 \times L$, to avoid the finite-size/temperature effect.

It is obvious that the $\langle m^2 \rangle$ remains a finite value of $J = 8$ and 9. The data of $J = 10$ resemble a straight line under double logarithmic axes, which is also another evidence for the critical point consistent to the Fig. 2. These results are also consistent with the phase diagram of the EH in Fig. 1(c): while the coupling ratio J becomes smaller, the critical temperature T_A rises higher. The ordered phase at low temperature of the EH is confirmed without any doubts, which also reflects the convinced finite-temperature phase transition of the EH. According to the symmetry analysis of the system, the EH must be constructed via SU(2) terms to keep its continuous symmetry. All the evidence now support this 2D phase transition of continuous symmetry breaking beyond the Mermin-Wagner theorem, which reveals the exist of relevant long-range terms.

C. Entanglement spectrum

The EH actually exhibits interactions that significantly deviate from those predicted by the well-known Li-Haldane-Poilblanc conjecture. The EH has a finite-temperature phase transition while the edge Hamiltonian has nothing. The remaining question becomes the following: How large is the difference between the entanglement spectrum and the edge energy spectrum in this case? Combined with the QMC calculation of the RDM and stochastic analytic continuation (SAC) [82,92–94],

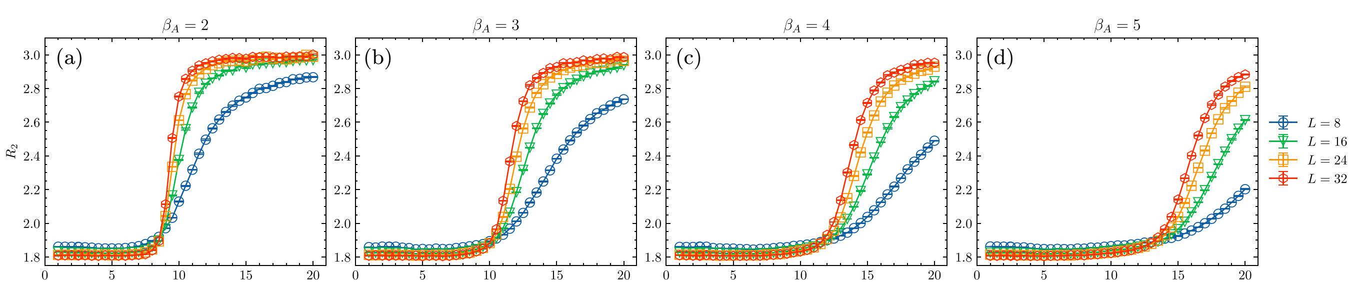

FIG. 3. The Binder ratio R_2 results at (a) $\beta_A = 2$, (b) $\beta_A = 3$, (c) $\beta_A = 4$, (d) $\beta_A = 5$, with a wide range sweeping of J from $J = 1$ to $J = 20$, and comparing the system size of $L = 8, 16, 24, 32$. These results suggest that a finite-temperature phase transition exists on EH.

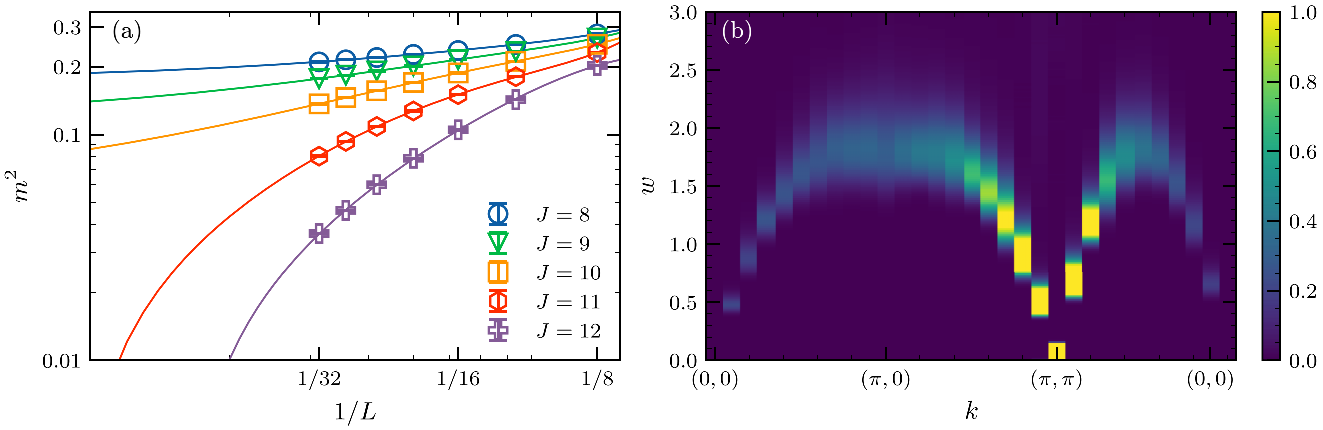

FIG. 4. (a) Finite-size scaling of m^2 under $\beta_A = 3$, with $J = 8, 9, 10, 11, 12$. All curves are fitted with a third-order polynomial and then extrapolated to nearing 0. The extrapolate shows a highly possible signal that there is a phase transition between $J = 10$ and $J = 11$. (b) Entanglement spectrum $S(\mathbf{k}, \omega)$ of a replicated $L = 20$ bilayer antiferromagnetic Heisenberg model with $\beta = 2 \times L$, $\beta_A = 50$ and $J = 10$. The maximum values of $S(\mathbf{k}, \omega)$ are truncated to 1.

we can obtain the entanglement spectrum using the scheme of Refs. [77,89–91]. As shown in Fig. 4(b), the entanglement spectrum seems still similar to a spin-wave excitation of a short-range Heisenberg model on a square lattice, i.e., the edge Hamiltonian. From this aspect, the entanglement spectrum approximately resembles the edge Hamiltonian, at least visually. That is, the relevant long-range interaction obviously changes the property of the physical system to induce a finite-temperature phase transition, but it still has not hugely modified the structure of the spectra information. It may be the main reason why such a difference between the EH and edge Hamiltonian has not been found in a long time.

V. CONCLUSION AND DISCUSSION

In this work, we find that, although the spectrum structures of the entanglement Hamiltonian and the edge Hamiltonian are almost similar, which obeys the Li-Haldane-Poilblanc conjecture, the actual properties of the two Hamiltonians are totally different. Taking the Heisenberg model on a bilayer square lattice as an example and setting one layer as the environment, the 2D entanglement Hamiltonian containing continuous symmetry exhibits a finite-temperature phase transition which violates the Mermin-Wagner theorem. Via designing the path-integral manifold of QMC, we simulated the finite-temperature property of the EH to strongly support the above conclusion. All the evidence points to the fact that there should be some necessary corrections with long-range interacting terms to the EH. From the spectra analysis, although the corrections hugely change the physical properties of the EH and make it totally different from the edge Hamiltonian, the two Hamiltonians' spectra are still seemly semblable.

We note that a gapless ground state with long-range entanglement may lead to a long-range EH in some analytic arguments [95,96]. A very recent theoretical work (almost the same time as ours) concluded a trivial gapped state (e.g., dimer phase) cannot hold a long-range EH [97] and the conclusion was demonstrated numerically in 1D systems [97,98]. In fact, our result provides an interesting counterexample in two dimensions, thus attracting further research.

ACKNOWLEDGMENTS

We acknowledge useful discussions with Zheng Zhou, Bin-Bin Chen, Meng Cheng, Xiao-Liang Qi, and Wei Zhu. We also appreciate the help from Weilun Jiang and Gaopei Pan. R.-Z.H is supported by a postdoctoral fellowship from the Special Research Fund (BOF) of Ghent University. Y.-M.D. and Z.Y. acknowledge the support from the start-up funding of Westlake University. Z.Y.M. thanks support from the RGC of Hong Kong SAR of China (Projects No. 17301420, No. 17301721, No. AoE/P-701/20, No. 17309822, and No. HKU C7037-22G), the ANR/RGC Joint Research Scheme sponsored by Research Grants Council of Hong Kong SAR of China and French National Research Agency (Project No. A_HKU703/22), the K. C. Wong Education Foundation (Grant No. GJTD-2020-01), and the Seed Funding "Quantum-Inspired explainable-AI" at the HKU-TCL Joint Research Centre for Artificial Intelligence. Y.-C.W. acknowledges support from the Zhejiang Provincial Natural Science Foundation of China (Grant No. LZ23A040003). We thank Beijng PARATERA Tech Co., Ltd., the Blackbody HPC system at the Department of Physics, University of Hong Kong for providing computational resources that contributed to the research results in this paper.

[1] G. Vidal, J. I. Latorre, E. Rico, and A. Kitaev, Entanglement in quantum critical phenomena, Phys. Rev. Lett. **90**, 227902 (2003).

[2] V. E. Korepin, Universality of entropy scaling in one dimensional gapless models, Phys. Rev. Lett. **92**, 096402 (2004).

[3] A. Kitaev and J. Preskill, Topological entanglement entropy, Phys. Rev. Lett. **96**, 110404 (2006).

[4] M. Levin and X.-G. Wen, Detecting topological order in a ground state wave function, Phys. Rev. Lett. **96**, 110405 (2006).

[5] P. Calabrese and A. Lefevre, Entanglement spectrum in one-dimensional systems, Phys. Rev. A **78**, 032329 (2008).

[6] E. Fradkin and J. E. Moore, Entanglement entropy of 2D conformal quantum critical points: Hearing the shape of a quantum drum, Phys. Rev. Lett. **97**, 050404 (2006).

[7] Z. Nussinov and G. Ortiz, Sufficient symmetry conditions for Topological quantum order, Proc. Natl. Acad. Sci. USA **106**, 16944 (2009).

[8] Z. Nussinov and G. Ortiz, A symmetry principle for topological quantum order, Ann. Phys. (NY) **324**, 977 (2009).

[9] H. Casini and M. Huerta, Universal terms for the entanglement entropy in 2 + 1 dimensions, Nucl. Phys. B **764**, 183 (2007).

[10] W. Ji and X.-G. Wen, Noninvertible anomalies and mapping-class-group transformation of anomalous partition functions, Phys. Rev. Res. **1**, 033054 (2019).

[11] W. Ji and X.-G. Wen, Categorical symmetry and noninvertible anomaly in symmetry-breaking and topological phase transitions, Phys. Rev. Res. **2**, 033417 (2020).

[12] L. Kong, T. Lan, X.-G. Wen, Z.-H. Zhang, and H. Zheng, Algebraic higher symmetry and categorical symmetry: A holographic and entanglement view of symmetry, Phys. Rev. Res. **2**, 043086 (2020).

[13] X.-C. Wu, W. Ji, and C. Xu, Categorical symmetries at criticality, J. Stat. Mech.: Theory Exp. (2021) 073101.

[14] X.-C. Wu, C.-M. Jian, and C. Xu, Universal features of higher-form symmetries at phase transitions, SciPost Phys. **11**, 033 (2021).

[15] J. Zhao, Y.-C. Wang, Z. Yan, M. Cheng, and Z. Y. Meng, Scaling of entanglement entropy at deconfined quantum criticality, Phys. Rev. Lett. **128**, 010601 (2022).

[16] J. Zhao, B.-B. Chen, Y.-C. Wang, Z. Yan, M. Cheng, and Z. Y. Meng, Measuring Rényi entanglement entropy with high efficiency and precision in quantum Monte Carlo simulations, npj Quantum Mater. **7**, 69 (2022).

[17] Y.-C. Wang, N. Ma, M. Cheng, and Z. Y. Meng, Scaling of the disorder operator at deconfined quantum criticality, SciPost Phys. **13**, 123 (2022).

[18] F. Pollmann, A. M. Turner, E. Berg, and M. Oshikawa, Entanglement spectrum of a topological phase in one dimension, Phys. Rev. B **81**, 064439 (2010).

[19] L. Fidkowski, Entanglement spectrum of topological insulators and superconductors, Phys. Rev. Lett. **104**, 130502 (2010).

[20] H. Yao and X.-L. Qi, Entanglement entropy and entanglement spectrum of the Kitaev model, Phys. Rev. Lett. **105**, 080501 (2010).

[21] X.-L. Qi, H. Katsura, and A. W. W. Ludwig, General relationship between the entanglement spectrum and the edge state spectrum of topological quantum states, Phys. Rev. Lett. **108**, 196402 (2012).

[22] E. Canovi, E. Ercolessi, P. Naldesi, L. Taddia, and D. Vodola, Dynamics of entanglement entropy and entanglement spectrum crossing a quantum phase transition, Phys. Rev. B **89**, 104303 (2014).

[23] D. J. Luitz, F. Alet, and N. Laflorencie, Universal behavior beyond multifractality in quantum many-body systems, Phys. Rev. Lett. **112**, 057203 (2014).

[24] D. J. Luitz, F. Alet, and N. Laflorencie, Shannon-rényi entropies and participation spectra across three-dimensional $O(3)$ criticality, Phys. Rev. B **89**, 165106 (2014).

[25] D. J. Luitz, N. Laflorencie, and F. Alet, Participation spectroscopy and entanglement Hamiltonian of quantum spin models, J. Stat. Mech.: Theory Exp. (2014) P08007.

[26] C.-M. Chung, L. Bonnes, P. Chen, and A. M. Läuchli, Entanglement spectroscopy using quantum Monte Carlo, Phys. Rev. B **89**, 195147 (2014).

[27] H. Pichler, G. Zhu, A. Seif, P. Zoller, and M. Hafezi, Measurement protocol for the entanglement spectrum of cold atoms, Phys. Rev. X **6**, 041033 (2016).

[28] J. I. Cirac, D. Poilblanc, N. Schuch, and F. Verstraete, Entanglement spectrum and boundary theories with projected entangled-pair states, Phys. Rev. B **83**, 245134 (2011).

[29] V. M. Stojanović, Entanglement-spectrum characterization of ground-state nonanalyticities in coupled excitation-phonon models, Phys. Rev. B **101**, 134301 (2020).

[30] W.-Z. Guo, Entanglement spectrum of geometric states, J. High Energy Phys. 02 (2021) 085.

[31] T. Grover, Entanglement of interacting fermions in quantum Monte Carlo calculations, Phys. Rev. Lett. **111**, 130402 (2013).

[32] F. F. Assaad, T. C. Lang, and F. Parisen Toldin, Entanglement spectra of interacting fermions in quantum Monte Carlo simulations, Phys. Rev. B **89**, 125121 (2014).

[33] F. F. Assaad, Stable quantum Monte Carlo simulations for entanglement spectra of interacting fermions, Phys. Rev. B **91**, 125146 (2015).

[34] F. Parisen Toldin and F. F. Assaad, Entanglement Hamiltonian of interacting fermionic models, Phys. Rev. Lett. **121**, 200602 (2018).

[35] X.-J. Yu, R.-Z. Huang, H.-H. Song, L. Xu, C. Ding, and L. Zhang, Conformal boundary conditions of symmetry-enriched quantum critical spin chains, Phys. Rev. Lett. **129**, 210601 (2022).

[36] Z. Moradi and J. Abouie, Entanglement spectrum of fermionic bilayer honeycomb lattice: Hofstadter butterfly, J. Stat. Mech.: Theory Exp. (2016) 113101.

[37] F. D. M. Haldane, Continuum dynamics of the 1-D Heisenberg antiferromagnet: Identification with the O(3) nonlinear sigma model, Phys. Lett. A **93**, 464 (1983).

[38] F. D. M. Haldane, Nonlinear field theory of large-spin Heisenberg antiferromagnets: Semiclassically quantized solitons of the one-dimensional easy-axis Néel state, Phys. Rev. Lett. **50**, 1153 (1983).

[39] H. Li and F. D. M. Haldane, Entanglement spectrum as a generalization of entanglement entropy: Identification of topological order in non-Abelian fractional quantum Hall effect states, Phys. Rev. Lett. **101**, 010504 (2008).

[40] D. Poilblanc, Entanglement spectra of quantum Heisenberg ladders, Phys. Rev. Lett. **105**, 077202 (2010).

[41] V. Alba, M. Haque, and A. M. Läuchli, Entanglement spectrum of the Heisenberg XXZ chain near the ferromagnetic point, J. Stat. Mech.: Theory Exp. (2012) P08011.

[42] V. Alba, M. Haque, and A. M. Läuchli, Entanglement spectrum of the two-dimensional Bose-Hubbard model, Phys. Rev. Lett. **110**, 260403 (2013).

[43] W. Zhu, Z. Huang, Y.-C. He, and X. Wen, Entanglement Hamiltonian of many-body dynamics in strongly correlated systems, Phys. Rev. Lett. **124**, 100605 (2020).

[44] W. Zhu, Z. Huang, and Y.-C. He, Reconstructing entanglement Hamiltonian via entanglement eigenstates, Phys. Rev. B **99**, 235109 (2019).

[45] Q.-C. Tang and W. Zhu, Critical scaling behaviors of entanglement spectra, Chin. Phys. Lett. **37**, 010301 (2020).

[46] T. Mendes-Santos, G. Giudici, R. Fazio, and M. Dalmonte, Measuring von Neumann entanglement entropies without wave functions, New J. Phys. **22**, 013044 (2020).

[47] M. Dalmonte, V. Eisler, M. Falconi, and B. Vermersch, Entanglement Hamiltonians: From field theory to lattice models and experiments, Ann. Phys. (Leipzig) **534**, 2200064 (2022).

[48] M. K. Joshi, C. Kokail, R. van Bijnen, F. Kranzl, T. V. Zache, R. Blatt, C. F. Roos, and P. Zoller, Exploring large-scale entanglement in quantum simulation, Nature (London) **624**, 539 (2023).

[49] Q. Redon, Q. Liu, J.-B. Bouhiron, N. Mittal, A. Fabre, R. Lopes, and S. Nascimbene, Realizing the entanglement Hamiltonian of a topological quantum Hall system, arXiv:2307.06251.

[50] M. Dalmonte, B. Vermersch, and P. Zoller, Quantum simulation and spectroscopy of entanglement Hamiltonians, Nat. Phys. **14**, 827 (2018).

[51] M. Ma, Y. Li, and J. Shang, Multipartite entanglement measures: a review, arXiv:2309.09459.

[52] V. Eisler, G. D. Giulio, E. Tonni, and I. Peschel, Entanglement Hamiltonians for non-critical quantum chains, J. Stat. Mech.: Theory Exp. (2020) 103102.

[53] M. Pouranvari and J. Abouie, Entanglement conductance as a characterization of a delocalized-localized phase transition in free fermion models, Phys. Rev. B **100**, 195109 (2019).

[54] J. Cardy and E. Tonni, Entanglement Hamiltonians in two-dimensional conformal field theory, J. Stat. Mech.: Theory Exp. (2016) 123103.

[55] N. Javerzat and E. Tonni, On the continuum limit of the entanglement Hamiltonian of a sphere for the free massless scalar field, J. High Energy Phys. 02 (2022) 086.

[56] V. Eisler, E. Tonni, and I. Peschel, On the continuum limit of the entanglement Hamiltonian, J. Stat. Mech.: Theory Exp. (2019) 073101.

[57] W.-J. Rao, X. Wan, and G.-M. Zhang, Critical-entanglement spectrum of one-dimensional symmetry-protected topological phases, Phys. Rev. B **90**, 075151 (2014).

[58] Y.-C. He, D. N. Sheng, and Y. Chen, Chiral spin liquid in a frustrated anisotropic kagome Heisenberg model, Phys. Rev. Lett. **112**, 137202 (2014).

[59] C. Fang, M. J. Gilbert, and B. A. Bernevig, Entanglement spectrum classification of C_n-invariant noninteracting topological insulators in two dimensions, Phys. Rev. B **87**, 035119 (2013).

[60] A. M. Läuchli and J. Schliemann, Entanglement spectra of coupled $s = \frac{1}{2}$ spin chains in a ladder geometry, Phys. Rev. B **85**, 054403 (2012).

[61] O. K. Diessel, S. Diehl, N. Defenu, A. Rosch, and A. Chiocchetta, Generalized Higgs mechanism in long-range-interacting quantum systems, Phys. Rev. Res. **5**, 033038 (2023).

[62] M. Song, J. Zhao, C. Zhou, and Z. Y. Meng, Dynamical properties of quantum many-body systems with long-range interactions, Phys. Rev. Res. **5**, 033046 (2023).

[63] A. Chiocchetta, D. Kiese, C. P. Zelle, F. Piazza, and S. Diehl, Cavity-induced quantum spin liquids, Nat. Commun. **12**, 5901 (2021).

[64] E. Yusuf, A. Joshi, and K. Yang, Spin waves in antiferromagnetic spin chains with long-range interactions, Phys. Rev. B **69**, 144412 (2004).

[65] N. Defenu, Metastability and discrete spectrum of long-range systems, Proc. Natl. Acad. Sci. USA **118**, e2101785118 (2021).

[66] S. Birnkammer, A. Bohrdt, F. Grusdt, and M. Knap, Characterizing topological excitations of a long-range Heisenberg model with trapped ions, Phys. Rev. B **105**, L241103 (2022).

[67] T. Horita, H. Suwa, and S. Todo, Upper and lower critical decay exponents of Ising ferromagnets with long-range interaction, Phys. Rev. E **95**, 012143 (2017).

[68] K. Fukui and S. Todo, Order-n cluster Monte Carlo method for spin systems with long-range interactions, J. Comput. Phys. **228**, 2629 (2009).

[69] N. D. Mermin and H. Wagner, Absence of ferromagnetism or antiferromagnetism in one- or two-dimensional isotropic Heisenberg models, Phys. Rev. Lett. **17**, 1133 (1966).

[70] N. D. Mermin, Absence of ordering in certain classical systems, J. Math. Phys. **8**, 1061 (1967).

[71] P. W. Anderson, An approximate quantum theory of the antiferromagnetic ground state, Phys. Rev. **86**, 694 (1952).

[72] T. Oguchi, Theory of spin-wave interactions in ferro- and antiferromagnetism, Phys. Rev. **117**, 117 (1960).

[73] H. Shao, Y. Q. Qin, S. Capponi, S. Chesi, Z. Y. Meng, and A. W. Sandvik, Nearly deconfined spinon excitations in the square-lattice spin-1/2 Heisenberg antiferromagnet, Phys. Rev. X **7**, 041072 (2017).

[74] C. Zhou, Z. Yan, H.-Q. Wu, K. Sun, O. A. Starykh, and Z. Y. Meng, Amplitude mode in quantum magnets via dimensional crossover, Phys. Rev. Lett. **126**, 227201 (2021).

[75] Z. Liu, J. Li, R.-Z. Huang, J. Li, Z. Yan, and D.-X. Yao, Bulk and edge dynamics of a two-dimensional Affleck-Kennedy-Lieb-Tasaki model, Phys. Rev. B **105**, 014418 (2022).

[76] A. Chandran, V. Khemani, and S. L. Sondhi, How universal is the entanglement spectrum? Phys. Rev. Lett. **113**, 060501 (2014).

[77] Z. Yan and Z. Y. Meng, Unlocking the general relationship between energy and entanglement spectra via the wormhole effect, Nat. Commun. **14**, 2360 (2023).

[78] L. Wang, K. S. D. Beach, and A. W. Sandvik, High-precision finite-size scaling analysis of the quantum-critical point of Heisenberg antiferromagnetic bilayers, Phys. Rev. B **73**, 014431 (2006).

[79] M. Lohöfer, T. Coletta, D. G. Joshi, F. F. Assaad, M. Vojta, S. Wessel, and F. Mila, Dynamical structure factors and excitation modes of the bilayer Heisenberg model, Phys. Rev. B **92**, 245137 (2015).

[80] J. Zhao, M. Song, Y. Qi, J. Rong, and Z. Y. Meng, Finite-temperature critical behaviors in 2D long-range quantum Heisenberg model, npj Quantum Mater. **8**, 59 (2023).

[81] M. Song, J. Zhao, Y. Qi, J. Rong, and Z. Y. Meng, Quantum criticality and entanglement for the two-dimensional long-range Heisenberg bilayer, Phys. Rev. B **109**, L081114 (2024).
[82] A. W. Sandvik, Stochastic method for analytic continuation of quantum Monte Carlo data, Phys. Rev. B **57**, 10287 (1998).
[83] A. W. Sandvik, Computational studies of quantum spin systems, AIP Conf. Proc. **1297**, 135 (2010).
[84] A. W. Sandvik and J. Kurkijärvi, Quantum Monte Carlo simulation method for spin systems, Phys. Rev. B **43**, 5950 (1991).
[85] A. W. Sandvik, Stochastic series expansion method with operator-loop update, Phys. Rev. B **59**, R14157 (1999).
[86] O. F. Syljuåsen and A. W. Sandvik, Quantum Monte Carlo with directed loops, Phys. Rev. E **66**, 046701 (2002).
[87] Z. Yan, Y. Wu, C. Liu, O. F. Syljuåsen, J. Lou, and Y. Chen, Sweeping cluster algorithm for quantum spin systems with strong geometric restrictions, Phys. Rev. B **99**, 165135 (2019).
[88] Z. Yan, Global scheme of sweeping cluster algorithm to sample among topological sectors, Phys. Rev. B **105**, 184432 (2022).
[89] Z. Liu, R.-Z. Huang, Z. Yan, and D.-X. Yao, Demonstrating the wormhole mechanism of the entanglement spectrum via a perturbed boundary, Phys. Rev. B **109**, 094416 (2024).
[90] S. Wu, X. Ran, B. Yin, Q.-F. Li, B.-B. Mao, Y.-C. Wang, and Z. Yan, Classical model emerges in quantum entanglement: Quantum Monte Carlo study for an Ising-Heisenberg bilayer, Phys. Rev. B **107**, 155121 (2023).
[91] M. Song, J. Zhao, Z. Yan, and Z. Y. Meng, Different temperature dependence for the edge and bulk of the entanglement Hamiltonian, Phys. Rev. B **108**, 075114 (2023).
[92] K. S. D. Beach, Identifying the maximum entropy method as a special limit of stochastic analytic continuation, arXiv:cond-mat/0403055.
[93] O. F. Syljuåsen, Using the average spectrum method to extract dynamics from quantum Monte Carlo simulations, Phys. Rev. B **78**, 174429 (2008).
[94] H. Shao and A. W. Sandvik, Phys. Rep. **1003**, 1 (2023).
[95] T. Yoshino, S. Furukawa, and M. Ueda, Intercomponent entanglement entropy and spectrum in binary Bose-Einstein condensates, Phys. Rev. A **103**, 043321 (2021).
[96] R. Lundgren, Y. Fuji, S. Furukawa, and M. Oshikawa, Entanglement spectra between coupled Tomonaga-Luttinger liquids: Applications to Ladder systems and topological phases, Phys. Rev. B **88**, 245137 (2013).
[97] Y.-N. Zhou, X. Li, H. Zhai, C. Li, and Y. Gu, Reviving the Lieb-Schultz-Mattis theorem in open quantum systems, arXiv:2310.01475.
[98] C. Li, X. Li, and Y.-N. Zhou, Numerical investigations of the extensive entanglement Hamiltonian in quantum spin ladders, Quantum Front **3**, 9 (2024).